Representation of Bay of Bengal Upper-Ocean Salinity in General Circulation Models

By Jasti S. Chowdary, G. Srinivas, T.S. Fousiya, Anant Parekh, C. Gnanaseelan, Hyodae Seo, and Jennifer A. MacKinnon

Photo credit: N, Suresh Kumar

> Representation of the Bay of Bengal salinity structure both in coupled and uncoupled (stand-alone) general circulation models has been challenging due to the complexity arising from the unique physical and dynamical processes in this basin.

ABSTRACT. The Bay of Bengal (BoB) upper-ocean salinity is examined in the National Centers for Environmental Prediction-Climate Forecasting System version 2 (CFSv2) coupled model, Modular Ocean Model version 5 (MOM5), and Indian National Centre for Ocean Information Services Global Ocean Data Assimilation System (INC-GODAS). CFSv2 displays a large positive salinity bias with respect to World Ocean Atlas 2013 in the upper 40 m of the water column. The prescribed annual mean river discharge and excess evaporation are the main contributors to the positive bias in surface salinity. Overestimation of salinity advection also contributes to the high surface salinity in the model during summer. The surface salinity bias in MOM5 is smaller than in CFSv2 due to prescribed local freshwater flux and seasonally varying river discharge. However, the bias is higher around 70 m in summer and 40 m in fall. This bias is attributed to excessive vertical mixing in the upper ocean. Despite the fact that representation of salinity in INC-GODAS is more realistic due to data assimilation, the vertical mixing scheme still imposes systematic errors. The small-scale processes that control oceanographic turbulence are not adequately resolved in any of these models. Better parameterizations based on dedicated observational programs may help improve freshwater representation in regional and global models.

INTRODUCTION

The Bay of Bengal (BoB) is a unique tropical basin whose physical properties exhibit extreme variability. This variability is governed by southwesterly monsoon winds from May to September and northeasterly monsoon winds from October to March (e.g., Schott and McCreary, 2001; Shankar et al., 2002). In the BoB, precipitation exceeds evaporation (e.g., Prasad, 1997), and adjoining rivers input a large amount of freshwater (e.g., Subramanian, 1993), making the upper ocean in this region substantially fresher compared to other tropical oceans (e.g., Sengupta et al., 2006). The low-salinity upper layers maintain stable stratification (Narvekar and Prasanna Kumar, 2006; Agarwal et al., 2012), which is largely controlled by surface freshwater fluxes (e.g., Sengupta et al., 2016; Wilson and Riser, 2016). In

general, sea surface temperature (SST) remains over 28°C in the BoB throughout the year, which is favorable for generation of active convection (Gadgil et al., 1984; Graham and Barnett, 1987; Sanilkumar et al., 1994). The shallow halocline and enhanced stratification in the upper ocean are known to maintain the high heat content and SST in the BoB (Shenoi et al., 2002, Mahadevan et al., 2016, in this issue). Further, such salinity structure influences the evolution of mixed layer temperature in regions of near-surface haline stratification (Rao and Sivakumar, 1999, 2003; Howden and Murtugudde, 2001; Kara et al., 2003; de Boyer Montégut et al., 2004).

Representation of the BoB salinity structure both in coupled and uncoupled (stand-alone) general circulation models (GCMs) has been challenging due to the

complexity arising from the unique physical and dynamical processes in this basin. The East India Coastal Current (EICC) is known to play an important role in maintaining the large-scale mass and salt balances between the BoB and the Arabian Sea (e.g., Durand et al., 2009). Studies suggest that the EICC transports freshwater southward along the east coast of India at the end of summer, and it reaches the southern tip of India by the end of boreal fall (e.g., Durand et al., 2009; Akhil et al., 2014). Apart from this, the winter monsoon current transports low-salinity BoB water to the Arabian Sea (Vinayachandran et al., 2005). Previous ocean model studies (e.g., Akhil et al., 2014) have suggested that erosion of the freshwater tongue along the east coast of India is due to vertical processes rather than horizontal advection. Furthermore, observations have revealed the importance of upward pumping of saltier water to the surface to maintain the salt balance in the southern BoB (Vinayachandran et al., 2013). This suggests the importance of both vertical and lateral processes in controlling the salinity budget in the BoB.

Thus, it is essential to properly represent freshwater flux, current systems, and vertical processes (e.g., Benshila et al., 2014; Akhil et al., 2014; Wilson and Riser, 2016; Parekh et al., 2016; Behara and Vinayachandran, 2016, and references therein) within GCMs so that they simulate realistic surface and subsurface salinity structure in the BoB. Previous modeling studies examined BoB surface salinity variability using sensitivity

experiments to understand the relative contributions of various processes (Thompson et al., 2006; Vinayachandran and Nanjundiah, 2009; Akhil et al., 2014; Rahaman et al., 2014). Many GCMs have positive sea surface salinity biases of 2–3 psu over the freshwater-dominated northern BoB. However, factors responsible for such salinity biases in the BoB (both in the surface and in the subsurface) are unclear and need examination. Biases in subsurface salinity and temperature in GCMs can alter the ocean circulation, sea level, vertical mixing, and the coupling between ocean and atmosphere (e.g., Seo et al., 2009; Brown et al., 2013). Thus, accurate representation of the vertical structure of salinity in GCMs is important.

In this study, characteristics and mechanisms of BoB upper-ocean (200 m) salinity biases are examined in multiple models to identify possible areas of model improvement for the BoB. Mechanisms responsible for salinity bias are investigated in the National Centers for Environmental Prediction (NCEP) Climate Forecast System (CFS) version 2 (CFSv2; Saha et al., 2014; a coupled GCM), Geophysical Fluid Dynamics Laboratory (GFDL) Modular Ocean Model version 5 (MOM5; Griffies, 2012; a stand-alone ocean model), and Indian National Centre for Ocean Information Services (INCOIS)-Global Ocean Data Assimilation System (INC-GODAS; Ravichandran et al., 2013; a data assimilation product; see Table 1 for details). This article describes details of different models and data sets used in the study, provides insights into salinity biases in the BoB vertical structure and associated processes, and discusses thoughts for future work.

MODELS AND DATA

NCEP-CFSv2 is a fully coupled ocean-atmosphere-land model with advanced physics and increased resolution compared to CFSv1 (Saha et al., 2006). Under the National Monsoon Mission of India, CFSv2 has been selected as an operational model for dynamical monsoon prediction over the Indian region (http://www.tropmet.res.in/monsoon/index.php); this model has also been widely used for global-scale forecasts (Saha et al., 2014). The Global Forecast System's (GFS) atmospheric component has a horizontal resolution of T126 (~100 km) and 64 sigma layers vertically (Saha et al., 2014). The ocean component of CFSv2 is the GFDL-MOM4 model (Griffies et al., 2004). CFSv2 is integrated over a period of 100 years. The last 60 years are utilized for preparing monthly climatology for the present study. More details of the CFSv2

TABLE 1. Forcing, vertical mixing schemes, and various fluxes used in CFSv2, MOM5, and INC-GODAS.

	CFSv2	MOM5	INC-GODAS
OGCM	GFDL-MOM4	Stand-alone OGCM	MOM4
Vertical mixing parameterization	Nonlocal K-profile parameterization (Large et al., 1994)	Nonlocal K-profile parameterization (Large et al., 1994)	Nonlocal K-profile parameterization (Large et al., 1994)
River runoff	Annual mean runoff (single time step; Dai and Trenberth, 2002)	Monthly climatology (Dai et al., 2009)	Interannual monthly river discharge (derived from data sets provided by Dai et al., 2009, and Papa et al., 2010)
Data assimilation technique	None	None	3D VAR (Derber and Rosati, 1989)
Variables assimilated	None	None	Temperature and salinity profiles from Argo, TAO/TRITON, RAMA, PIRATA, XBT, CTD, and NDPB (Ravichandran et al., 2013)
Evaporation (E)	Computed from bulk formula using model SST and moisture from atmospheric model (GFS)	Computed from bulk formula using model SST (COREv2)	Computed from bulk formula using model SST
Precipitation (P)	Simulated by the GFS through Arakawa–Schubert (SAS) scheme (Pan and Wu, 1995)	Prescribed monthly mean precipitation from COREv2 (Large and Yeager, 2008)	Prescribed from monthly NCEP-R2 precipitation (Kanamitsu et al., 2002)
Wind forcing	Simulated by the GFS	Six-hourly winds from COREv2	QuikSCAT/DASCAT winds
Model domain and time period	Global and last 60 years of 100 years free run is used	Indo-Pacific region (30°E to 70°W, 60°S to 30°N); one hundred years spinup and interannual simulation from 1948 to 2008	Global and time period of 2003–2012
Horizontal and vertical resolution	Horizontally 0.5° × 0.5° and vertically 10 m in the upper 220 m	Horizontally 0.25° × 0.25° and vertically 10 m in the upper 220 m.	0.5° degree in zonal and meridional; meridional resolution is 0.25° within 10°S to 10°N and vertical resolution is 10 m in the upper 220 m
Radiation fluxes	RRTM (Rapid Radiative Transfer Mode) radiation scheme	Daily fluxes from COREv2	Daily NCEP-R2 fluxes

free run are provided in Roxy (2014).

The stand-alone ocean model MOM5 is forced with the Coordinated Ocean-ice Reference Experiments version 2 (COREv2) surface forcing data sets for global ocean-ice modeling (Large and Yeager, 2004), developed at the National Center for Atmospheric Research (NCAR). In the model, turbulent heat fluxes are derived from the NCAR bulk formulae using the simulated SST and the prescribed 10 m atmospheric parameters (see Table 1 for details). Monthly climatological river discharge at discrete river mouth locations at 1° × 1° global grid (Dai and Trenberth, 2002) is used.

Finally, ocean reanalysis generated by INC-GODAS is also examined (Ravichandran et al., 2013). INC-GODAS (ocean model is MOM4) is an improved version of NCEP-GODAS (ocean model is MOM3) with a shorter assimilation window (Ravichandran et al., 2013). Temperature and salinity profiles are assimilated at six-hour intervals using all observations from the 10-day assimilation window, and the 3DVAR assimilation technique is used for data assimilation. Temperature and salinity profiles are assimilated from various in situ ocean observational networks, including Argo profiling floats, Tropical Atmosphere Ocean/Triangle Trans-Ocean Buoy Network (TAO/TRITON; McPhaden, 1993), Research Moored Array for African-Asian-Australian Monsoon Analysis and Prediction (RAMA; McPhaden et al., 2009), Pilot Research Moored Array in the Atlantic (PIRATA; Servain et al., 1998) moored buoys, expendable bathythermographs (XBTs), and National Data Buoy Program (NDBP) moorings. We note that maintaining such varied observational networks (Venkatesan et al., 2013) is crucial if models are to be substantially constrained by data assimilation. Ravichandran et al. (2013) provide more details of INC-GODAS. The model is forced by momentum flux, heat flux, and freshwater flux from the NCEP-DOE atmospheric reanalysis

version 2 (Kanamitsu et al., 2002; hereafter, NCEP R2). INC-GODAS provides three-dimensional ocean structures and is currently being used to provide initial ocean conditions for the operational model CFSv2 for both seasonal and extended range prediction of the Indian summer monsoon (e.g., Sahai et al., 2013).

Vertical mixing in all three models is prescribed using the standard K-profile parameterization (KPP). The KPP scheme (Large et al., 1994) is one of the most widely used parameterization schemes for vertical mixing in ocean GCMs. Unlike bulk mixed layer models, KPP does not assume a well-mixed boundary layer and explicitly predicts an ocean boundary layer depth. Within this boundary layer, the turbulent mixing is parameterized using a nonlocal bulk Richardson number and similarity theory. Below the boundary layer, KPP invokes eddy coefficients to parameterize vertical mixing due to shear instability (when model resolved shear produces small Richardson numbers), breaking of a background internal wave field (assumed to be constant and quite weak), and double diffusion. Table 1 provides details about forcing and specifications of mixing schemes for the three models used in the present study.

The simulated fields from the three models, CFSv2, MOM5, and INC-GODAS, are compared with World Ocean Atlas 2013 (WOA13) temperature and salinity products (Locarnini et al., 2013; Zweng et al., 2013). The latter is a reasonable choice, as it has been found to be consistent with RAMA buoy data (not shown) and Argo data (Fousiya et al., 2015). We also consider the Estimating the Circulation and Climate of the Ocean, Phase II (ECCO2; Menemenlis et al., 2008) reanalysis data, the TropFlux air-sea flux product (Praveen Kumar et al., 2010), and Global Precipitation Climatology Project (GPCP) monthly precipitation data (Adler et al., 2003). The ECCO2 product is used in the present study to estimate circulation bias in the models. It

is an automatic differentiation tool that is used to calculate the adjoint code of MITgcm (Marshall et al., 1997; Azaneu et al., 2014). ECCO2 climatology is constructed from the period 1992–2007.

In the present study, the three models (CFSv2, MOM5, and INC-GODAS) are validated against the three data sets (WOA13, ECCO2, and TropFlux). To examine the causes for the salinity biases in these models, we compare the Brunt-Vaisala frequency (N^2; Gill, 1982), vertical shear of horizontal currents, and energy required for mixing (ERM). The latter is a metric of the potential energy of the upper water column (Shenoi et al., 2002). ERM is computed as

$$\text{ERM} = \tfrac{1}{8}\left(\rho_b - \rho_s\right)gh^2,$$

where g is acceleration due to gravity (9.8 m s^{-2}), ρ_s is surface layer density (kg m^{-3}), ρ_b is density at any particular depth beneath the surface mixed layer (kg m^{-3}), and h is mixed layer depth (m). ERM is a proxy for upper-ocean stratification.

UPPER-OCEAN SALINITY BIASES AND POSSIBLE CAUSES

Figure 1 shows depth-latitude sections of simulated salinity in CFSv2, MOM5, and INC-GODAS for all seasons, as well as the annual mean and salinity biases (with respect to WOA13) averaged over the BoB (85°E–90°E). CFSv2 shows very high salinity in the upper 20 m north of 14°N for all seasons. The salinity bias is particularly strong in summer (June through September) and fall (October and November), compared to WOA13 climatology (Figure 1c,d). The difference between the orientation of isohalines in CFSv2 (model) and WOA13 (data) illustrates discrepancies in salinity structure, clearly suggesting that the spatial distribution of freshwater is not well represented in the model. Salinity is more biased to the south of 14°N from the surface to 100 m depth in all seasons except spring (March through May). The model salinity is biased low around 40 m depth during fall and winter (December

through February). MOM5 shows low salinity in the upper 20 m of the northern BoB from March-April-May to October-November (Figure 1f–j). On the other hand, the southern BoB shows a weak bias in MOM5, unlike in CFSv2. However, there is anomalously low salinity in the region north of 16°N between 20 m and 60 m depth, with minimum bias in spring and maximum bias in fall (Figure 1g,i). The salinity representation in INC-GODAS is somewhat similar to MOM5 (Figure 1k–o). The seasonally varying river discharge prescribed in MOM5 and the assimilation of salinity profiles in INC-GODAS are likely the main factors for the slightly reduced surface salinity biases compared to CFSv2. However, there are still considerable biases in both models during boreal summer and fall. Further in-depth analysis is therefore performed to understand salinity biases in these models during summer and fall over the BoB.

Figure 2 shows vertical profiles of temperature, salinity, and density during boreal summer and fall, averaged over the BoB for CFSv2, MOM5, and INC-GODAS and compared with WOA13. In general, the temperature is high near the surface and decreases with depth and vice versa for salinity and density. However, upper-ocean salinity in the BoB is much lower
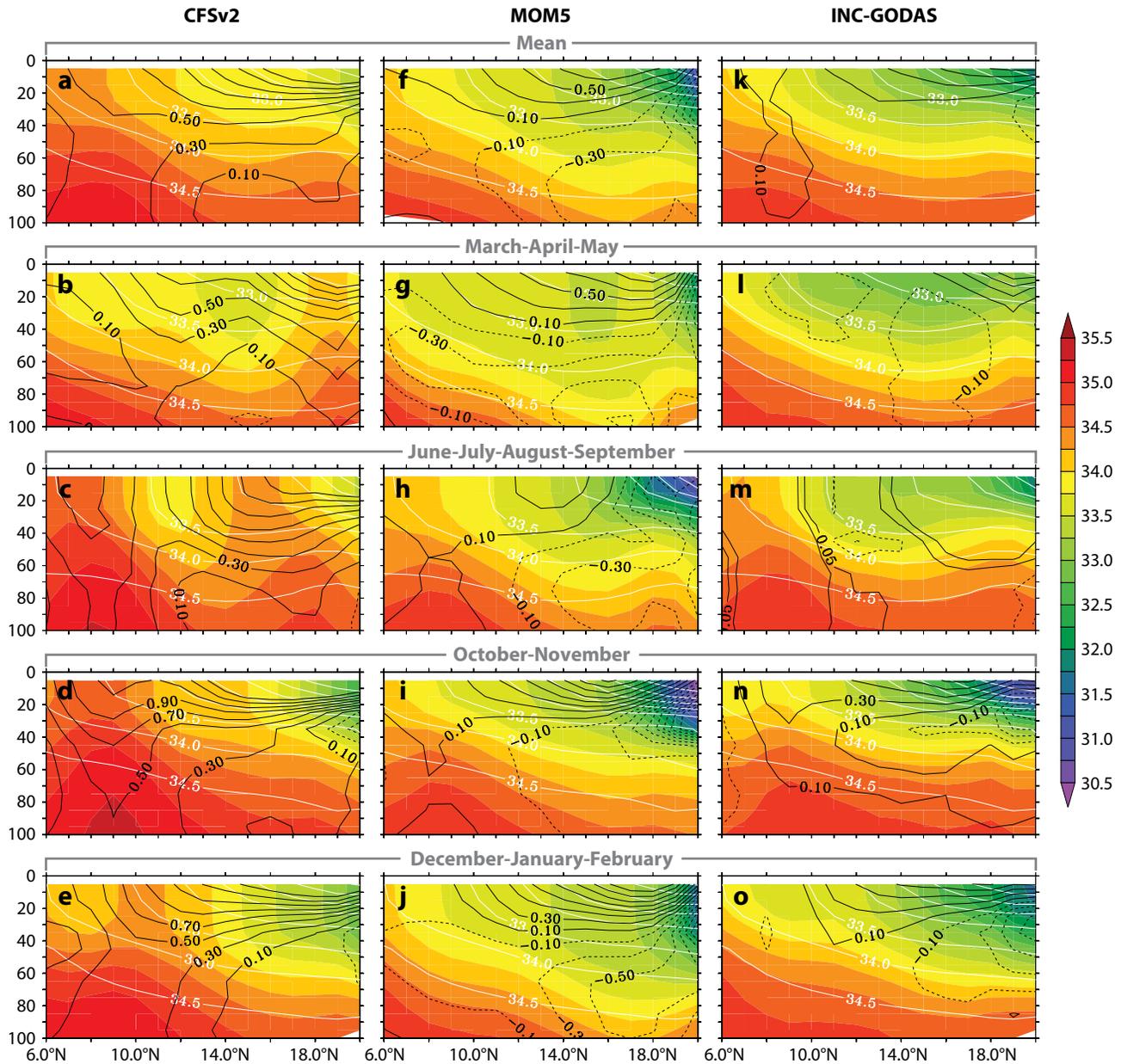

FIGURE 1. Depth-latitude plots of salinity (mean; shaded, psu) and bias (black contours, psu) averaged between 85°E and 90°E over the Bay of Bengal region in National Centers for Environmental Prediction-Climate Forecast System version 2 (CFSv2; left column), Modular Ocean Model version-5 (MOM5; middle column), and Indian National Centre for Ocean Information Services Global Ocean Data Assimilation System (INC-GODAS; right column) for annual mean (a, f, k), March-April-May (b, g, l), June-July-August-September (c, h, m), October-November (d, i, n), and December-January-February (e, j, o). Biases are calculated with respect to World Ocean Atlas 2013 (WOA13). White contours represent the WOA13 salinity.

FIGURE 2. Area averaged Bay of Bengal vertical profiles of (a) temperature (°C), (b) salinity (psu), and (c) density (kg m^{-3}) for CFSv2, MOM5, INC-GODAS, and WOA13 during summer (June-July-August-September). (d–f) Plots show respective biases. Similar to June through September, October-November vertical profiles of temperature, salinity, and density and their biases are displayed in (g) to (l). Vertical profiles are displayed for the upper 100 m. Bias is calculated with respect to WOA13.

than in the rest of the tropical Indian Ocean due to the large freshwater influx. CFSv2 displays a large cold bias for the upper 80 m of the water column, a positive bias in salinity from the surface to 100 m depth, and a positive bias in density up to 60 m depth (Figure 2d). In MOM5, the temperature bias is smaller, but salinity and density show a strong negative bias around 70 m depth. In the case of INC-GODAS, biases in temperature and density are high above 60 m (Figure 2f). During fall, the maximum positive bias in salinity is noted around 40 m in MOM5 and CFSv2 and negative bias in INC-GODAS (Figure 2j–l). Biases in temperature, salinity, and density are higher in fall compared to summer.

We next examine freshwater fluxes, water column stability, and current profiles in the upper ocean in order to investigate the causes of the biases. Figure 3a shows WOA13 climatology and CFSv2 vertical profiles of the Brunt-Vaisala frequency (N^2) averaged over the BoB for summer. CFSv2 displays a too-weak stability for the upper 100 m as compared

FIGURE 3. Vertical profiles for summer (June through September) (a) Brunt-Vaisala frequency (N^2; in 10^{-2} s^{-2}), (b) energy required for mixing (ERM; J m^{-2}), and (c) square of the vertical shear of horizontal currents (in 10^{-4} s^{-2}) averaged over the Bay of Bengal region (80°E–100°E, 6°N–23°N). (d–f) are the same as (a–c) but for normalized biases. Biases in N^2 and ERM (d,e) are calculated with respect to WOA13, whereas bias in vertical shear (f) is calculated with respect to Estimating the Circulation and Climate of the Ocean, Phase II (ECCO2). N^2 and ERM (vertical shear) biases are normalized with respect to WOA13 (ECCO2) and provided as percentage values.
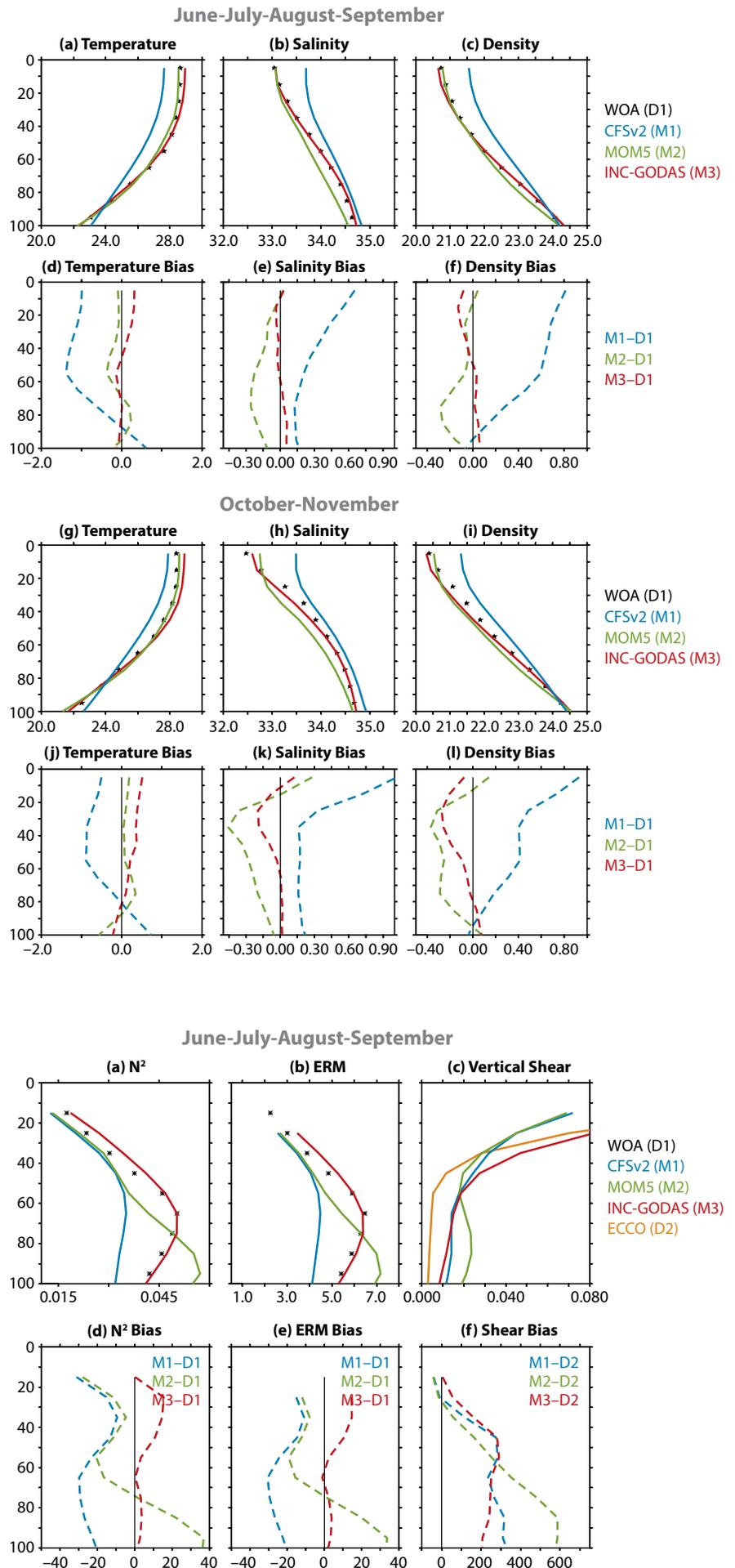
to WOA13, which is clearly seen in the bias (Figure 3d). The ERM profile is consistent with that for the entire tropical Indian Ocean (Chowdary et al., 2016b) and confirms the weak stability in CFSv2 (Figure 3b,e). Though upper-ocean salinity is better represented in MOM5 compared to CFSv2, the stability is still too weak in the top 60 m of the water column (Figure 3d,e). In the case of INC-GODAS, the stability is slightly higher than observed and is

better represented compared to CFSv2 and MOM5. This is mainly due to the assimilation of both temperature and salinity profiles. Figure 3c shows vertical shear of horizontal currents in CFSv2, MOM5, and INC-GODAS. Shear bias is calculated with respect to the ECCO2 product. It is evident from the bias that vertical shear is higher in all models compared to ECCO2 (Figure 3f). Strong vertical shear and weak stratification favors excessive mixing of low-salinity

surface water with subsurface water. This strong mixing should at least partially explain the salinity bias in both CFSv2 and MOM5. Low-salinity surface water in MOM5 is mixed down below 20 m, resulting in a negative bias around 40 m to 70 m in both the seasons. In the case of CFSv2, biases are consistent with excessive mixing, bringing cold, saline water upward and resulting in a positive bias in temperature below 80 m and a reduced bias in salinity below 60 m (Figure 2d,e). This prescribed mixing is likely triggered by subcritical Richardson numbers, due to a combination of high shear and low stratification in the model. Though INC-GODAS shows strong vertical shear, higher stability compared to other models limits KPP vertical mixing and hence helps to maintain a more realistic vertical salinity distribution in the BoB.

Figure 4 shows evaporation (E) minus precipitation (P) in CFSv2, MOM5, and INC-GODAS and their biases over the BoB during summer and fall. The east-west gradient in E−P is too strong in CFSv2 compared to observations in both summer and fall. Excess precipitation over evaporation is apparent along the Myanmar coast in CFSv2 during summer, a bias that has also been reported in earlier studies (e.g., Parekh et al., 2016; Chowdary et al., 2016a). However, precipitation in general is underestimated over most of the BoB, which arises from the biased rainfall simulation from the GFS. This strong positive E−P in the model would contribute to the high salinity bias, especially in the surface layer of the BoB in CFSv2 (Figure 2e). Similarly, CFSv2 displays a positive bias in freshwater flux during fall, which is responsible for the positive surface salinity bias (Figure 2k). Consistent with other coupled model studies, precipitation in the atmospheric component of CFSv2 contains strong biases, with overestimation of evaporation resulting in poor representation of surface salinity in the BoB (e.g., Seo et al., 2009). MOM5 displays a weak bias in E−P, which is reflected in a weak positive bias in surface salinity
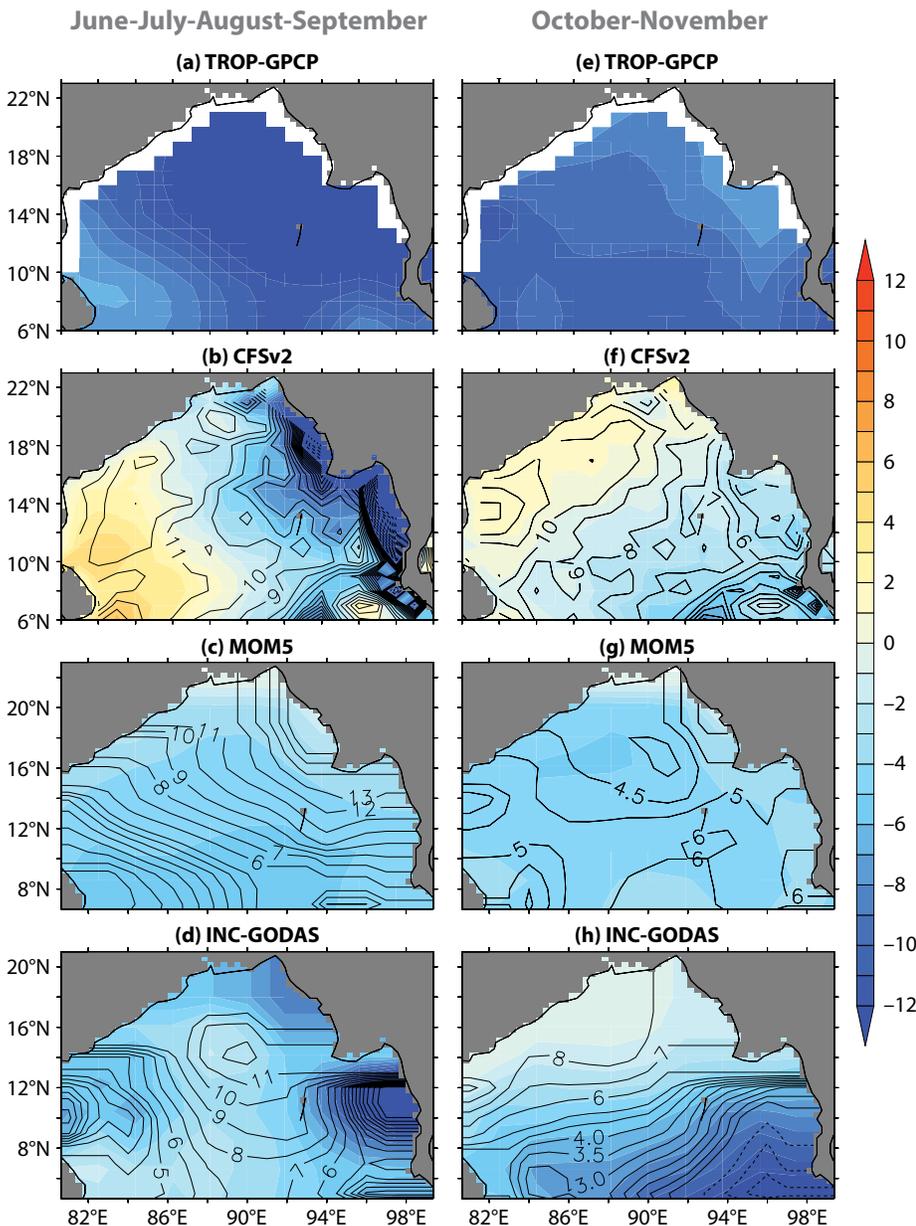

FIGURE 4. Evaporation minus precipitation (shaded; mm day⁻¹) and bias (contours) during summer (June-July-August-September) for (a) TropFlux and Global Precipitation Climatology Project monthly precipitation (GPCP) data products, (b) CFSv2, (c) MOM5, and (d) INC-GODAS. (e–h) The same as (a–d) but for fall (October-November) season.

(Figures 4c and 2e). INC-GODAS also shows a weak positive bias in E–P in most of the area during both summer and fall (Figure 4c). Evaporation changes in both models are partly dependent on simulated SSTs. In response to positive bias in E–P, INC-GODAS shows a weak positive surface salinity bias (Figure 2e). The weak biases in INC-GODAS and MOM5 are partly due to high evaporation, while the strong bias in CFSv2 is due to the bias in the model rainfall. Therefore, accurate representation of the net freshwater flux in the coupled models is critical for maintaining a more realistic upper-ocean salinity structure over the BoB, especially at the surface.

Horizontal advection is found to be important for salinity variations in the BoB for most of the year (e.g., Rao and Sivakumar, 2003; Sengupta et al., 2016, and references therein). During summer, ECCO2 shows some regions of northeastward or southeastward surface current averaged for the upper 40 m in the BoB (Figure 5a); these are consistent with Ekman transport by southwesterly monsoonal winds as an important component of average flow. The southward component of the surface current is weak in all models west of 86°E (Figure 5b–d). Westward current bias in the central BoB is particularly strong in CFSv2 and MOM5 and slightly weak in INC-GODAS, suggesting weaker eastward mean flows in all models. This may also reflect a failure to properly capture the surface-confined Ekman transports. During fall, a basin-scale cyclonic gyre is seen in ECCO2 surface currents (Figure 5e). The southward current component near the east coast of India (EICC) is strong in ECCO2 but is weaker in CFSv2, MOM5, and INC-GODAS (Figure 5f–h). Coastal current systems such as the EICC are not very well captured in models, mainly due to their coarser resolution. Overall, a too-weak cyclonic gyre during fall is evident in many models compared to ECCO2. Figure 6 illustrates mean meridional salinity advection at the southern boundary of the BoB (10°N) averaged from

85°E–90°E. As compared to ECCO2, during summer, CFSv2 overestimates salinity advection due to monsoon currents at the surface and in the subsurface (Figure 6a,b). This is consistent with the salinity biases in CFSv2 during summer (Figure 2). MOM5 also displays positive biases in salinity advection but bias is weaker (Figure 6c). In INC-GODAS, the strong negative bias in salinity advection in the upper ocean during spring and positive bias during summer are apparent

(Figure 6d). Discrepancies in salinity advection or inflow and outflow of saline water from the BoB in GCMs also contribute to the salinity bias.

DISCUSSION

The model salinity bias in the BoB could be due to a combination of inaccurate river forcing or freshwater forcing and the incorrect physical representation of the mixing. Our analysis reveals that the salinity bias, especially in the subsurface,
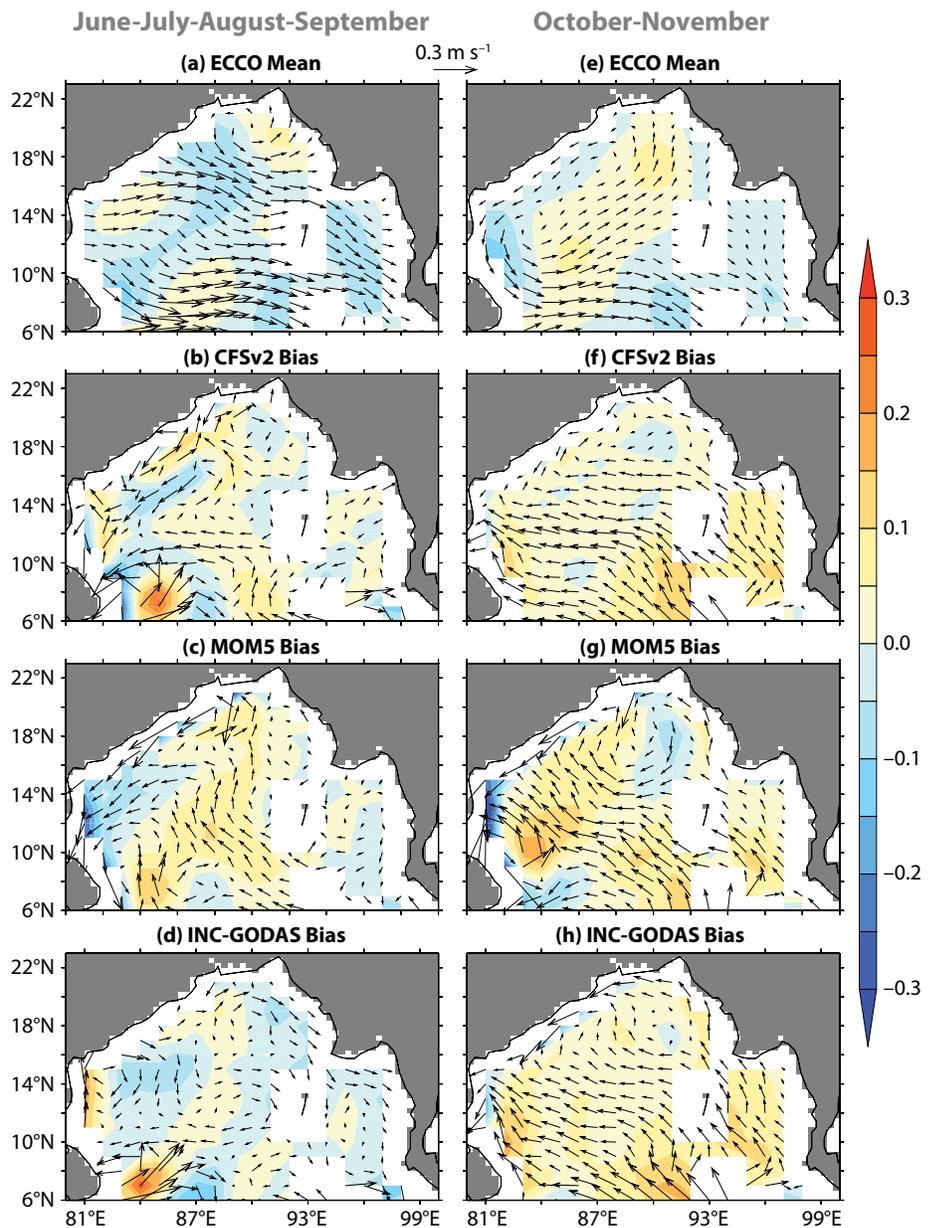

FIGURE 5. JJAS (a) mean ECCO2 surface currents (vectors, m s⁻¹) and mean meridional current (shaded, m s⁻¹), (b) bias in CFSv2 surface currents (vectors, m s⁻¹) and mean meridional current (shaded, m s⁻¹), (c) bias in MOM5, and (d) bias in INC-GODAS. (e–h) The same as (a–d) but for October-November (fall season).

does not arise primarily from the misrepresentation of river discharge. For example, we considered models with mean annual (CFSv2) and mean seasonal (MOM5, INC-GODAS) varying river discharges, but all three models show similar biases in subsurface structure, suggesting improper vertical mixing in these models is a likely culprit.

Although the stand-alone model (MOM5) was forced with seasonally varying river discharge data, there is no significant reduction in salinity biases, as anticipated by previous modeling studies (e.g., Durand et al., 2011). This issue is important and warrants further investigation. Because river discharges are a result of complex estuarine dynamics that are absent in ocean models, a dedicated observational campaign and sensitivity studies are needed to improve understanding of freshwater forcing due to river discharge (e.g., Mahadevan et al., 2016, in this issue). For example, river insertion

thickness in the ocean models might be a major factor, as it represents the thickness of the water column into which tracers from rivers are inserted. Tracer insertion is usually done in the mixed layer, so any misrepresentation of mixed layer thickness in the models would result in unrealistic insertion of river water. Another potentially important problem is inability to treat river water properties such as temperature, salinity, and turbidity. Of course, it is of utmost importance to develop better river discharge data at higher temporal resolution. When combined with in situ observations, satellite altimetry products can be useful for estimating river discharges at higher temporal frequency. Overall, a lack of accurate estimates of river runoff (amount, time scale, and properties) has resulted in a lack of consensus in the modeling community on the specification of river runoff; this remains the key challenge for numerical modeling of BoB circulation.

Ocean models with vertical shear parameterizations can successfully reproduce many general features of the tropical ocean (Packnowski and Philander, 1981). However, the BoB has several unusual features that may influence both the balance of dynamics that set turbulent mixing rates and upper-ocean stratification and the most appropriate parameterization strategies. There are two categories of concern here: ways in which KPP does not accurately represent the in situ vertical mixing processes, and processes that are simply not included or represented in existing models. In the former category of concern, one of the primary issues is resolution. In the BoB, many of the observed freshwater layers are on the order of 10 m thick or even thinner (Lucas et al., 2016, in this issue); models that have a 10 m vertical resolution will never be able to represent such layers accurately, and will always mix "too much." High priority should be thus given to increasing vertical
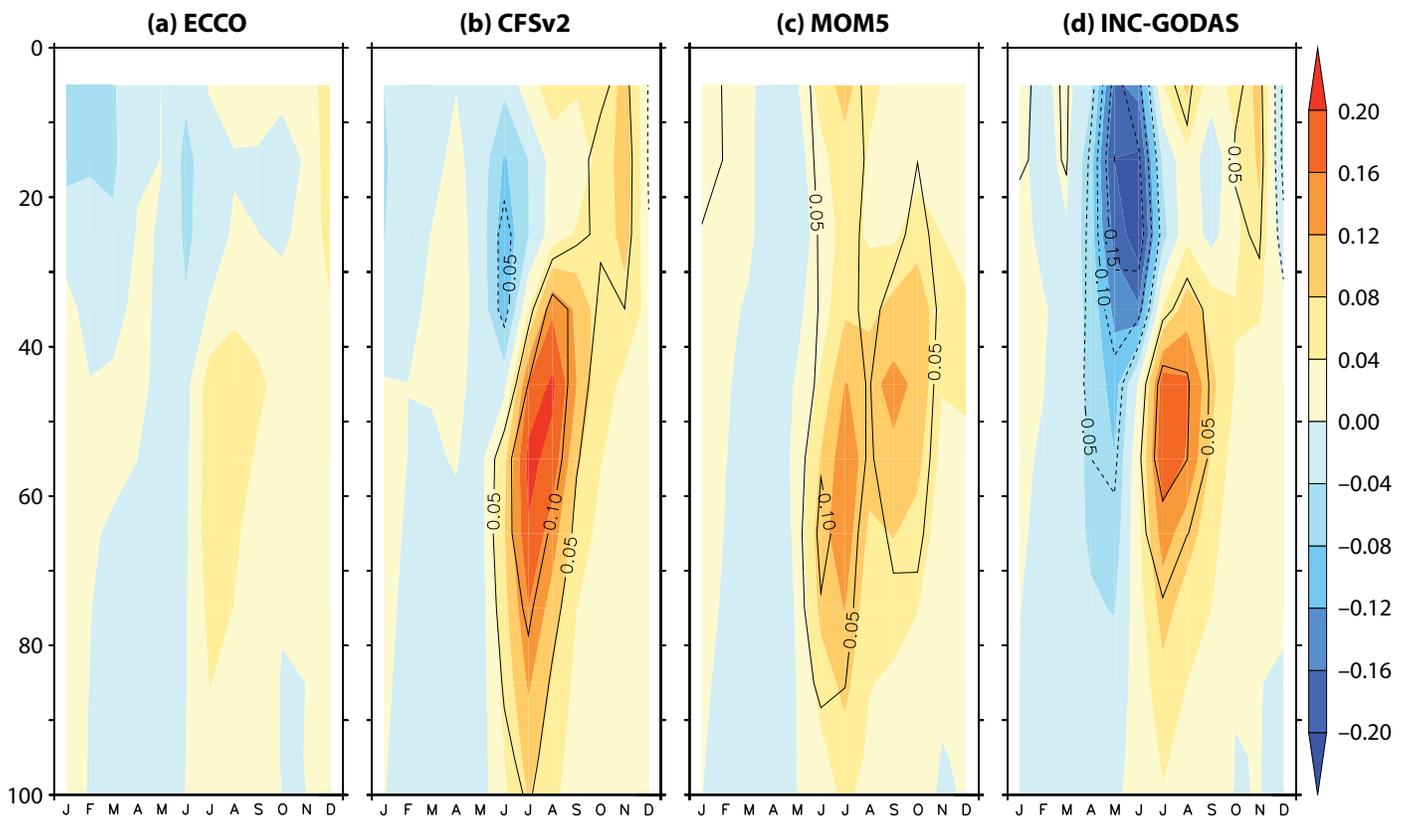

FIGURE 6. Monthly mean meridional salinity advection in the upper 100 m (shaded, in 10^{-6} psu s^{-1}) at the southern boundary of the Bay of Bengal (10°N) averaged from 85°E to 90°E. (a) ECCO2, (b) CFSv2, (c) MOM5, and (d) INC-GODAS. Contours in (b–d) represent bias.

resolution in the upper ocean for operational forecast models. Additionally, even with sufficient resolution, it is not clear that KPP, tuned for weaker stratification, will accurately represent entrainment and erosion at the extremely sharp haloclines found in the upper BoB in certain seasons (Lucas et al. and Jinadasa et al., 2016, both in this issue; Sengupta et al., 2016). Finally, KPP does not include a variety of vertical mixing processes, such as Langmuir turbulence, and this is likely important in mixing both scalers and momentum, though efforts are underway to remedy that omission.

In the second category of concern, which is accurate representation of in situ vertical mixing, a recent observational campaign and numerical process study have highlighted the importance of a variety of fundamentally three-dimensional phenomena that may play important roles in setting stratification but are not generally represented in the current generation of GCMs. Much of the surface layer in the BoB is freshwater stratified, so subject to the "interior ocean mixing" portion of KPP. Internal wave breaking in this layer is likely much more related to locally wind-generated near-inertial internal waves than the background levels assumed in KPP (Johnston et al., 2016, in this issue), and needs to be parameterized differently. A recent approach developed by Jochum et al. (2013) to explicitly include the effects of near-inertial motions for upper-ocean mixing in the tropics has shown great promise. In general, the shear that produces subcritical Richardson numbers in the ocean is almost never directly related to the types of mesoscale features resolved by the models presented here; it is instead related to internal waves, internal tides, and frontal processes, each of which must be properly parameterized (MacKinnon et al., 2013).

Many of the observations strongly suggest submesoscale instabilities (see Lucas et al. and Sarkar et al., 2016, both in this issue; Wijesekera et al., in press).

At times, such instabilities induce significant subduction of one water mass beneath another, increasing local stratification and inhibiting vertical mixing; lack of inclusion of such re-stratifying processes may be one reason for the low stratification/high mixing model biases reported here. Many submesoscale instabilities preferentially occur at sharp lateral density fronts, of the sort not explicitly resolved by the models considered here; hence, their effects must be parameterized in a different manner. Fox-Kemper et al. (2008a,b, 2011) parameterized one element in this family of restratifying processes; however, it is not yet clear whether the particular baroclinic instability represented in that scheme is prevalent in the BoB. Ongoing close collaboration between observationalists, process modelers, and the GCM community, of the sort facilitated by the Air-Sea Interactions Regional Initiative–Ocean Mixing and Monsoon (ASIRI-OMM) experiments, is imperative for development of the next generation of successful forecast models for the Bay of Bengal.

SUMMARY

Upper-ocean stratification in the Bay of Bengal is highly dependent upon salinity, which is substantially lower to the north of 14°N than to the south. Representation of BoB salinity in GCMs is challenging because of the complex ocean processes that need to be accurately captured by the models. In this study, we examined the seasonal mean biases in BoB upper-ocean structure, with a focus on salinity fields, in a coupled model (CFSv2), an ocean model (MOM5), and a reanalysis product (INC-GODAS) during summer and fall. A positive salinity bias of about 1 psu is noted north of 14°N in the BoB in CFSv2 over the upper 20 m of the water column. Area-averaged salinity over the BoB is high up to 100 m depth, and there is a maximum bias at the surface. At the same time, the temperature bias is negative. In MOM5, a negative (weakly positive) bias in salinity and density around

70 m (at the surface) is noted, and temperature bias is low. The INC-GODAS product displays relatively low bias in temperature and salinity compared to CFSv2 and MOM5.

The processes responsible for upper-ocean salinity biases such as freshwater flux, vertical mixing, and horizontal advection were examined in all models. Excessive evaporation over precipitation and prescribed annual mean river discharge in CFSv2 are mainly responsible for the positive salinity bias. MOM5 showed low-salinity bias in the upper 30 m, and this could be due to seasonally varying river discharge and prescribed E–P forcing. However, the salinity bias is higher in the subsurface at around 80 m in summer and 40 m in fall. Salinity is better represented in INC-GODAS in the upper 100 m over the BoB, due to assimilation of temperature and salinity profiles from Argo and other observations. CFSv2 and MOM5 show weaker stability with positive bias in density within the top few meters. Furthermore, in both models, vertical shear of the horizontal current is higher compared to ECCO2. This suggests excess mixing of low-salinity water from the surface with subsurface water in MOM5. In the model, a low Richardson number triggers excess vertical mixing. INC-GODAS salinity is better represented over BoB, but vertical shear of horizontal currents is not well captured. Furthermore, advection of high-salinity water in CFSv2 at the southern boundary of the BoB is consistent with the high-salinity bias. In MOM5, the salinity advection bias is weaker, and the converse is true for INC-GODAS. These results suggest that treatment of the river forcing (vertical mixing, freshwater flux, and lateral advection) is an important factor for improving representation of the BoB salinity fields in coupled and stand-alone ocean models. To estimate biases accurately, high-frequency spatiotemporal observations over the BoB from field campaigns such as those described in this volume would be very useful.

REFERENCES

Adler, R.F., G.J. Huffman, A. Chang, R. Ferraro, P. Xie, J. Janowiak, B. Rudolf, U. Schneider, S. Curtis, D. Bolvin, and others. 2003. The Version 2 Global Precipitation Climatology Project (GPCP) Monthly Precipitation Analysis (1979–present). *Journal of Hydrometeorology* 4:1,147–1,167, http://dx.doi.org/10.1175/1525-7541(2003)004<1147:TVGPCP>2.0.CO;2.

Agarwal, N., R. Sharma, A. Parekh, S. Basu, A. Sarkar, and V.K. Agarwal. 2012. Argo observations of barrier layer in the tropical Indian Ocean. *Advances in Space Research* 50:642–654, http://dx.doi.org/10.1016/j.asr.2012.05.021.

Akhil, V.P., F. Durand, M. Lengaigne, J. Vialard, M.G. Keerthi, V.V. Gopalakrishna, C. Deltel, F. Papa, and C. de Boyer Montégut. 2014. A modeling study of the processes of surface salinity seasonal cycle in the Bay of Bengal. *Journal of Geophysical Research* 119:3,926–3,947, http://dx.doi.org/10.1002/2013JC009632.

Azaneu, M., R. Kerr, and M. Mata. 2014. Assessment of the representation of Antarctic Bottom Water properties in the ECCO2 reanalysis. *Ocean Science* 10:923–946, http://dx.doi.org/10.5194/os-10-923-2014.

Behara, A., and P.N. Vinayachandran. 2016. An OGCM study of the impact of rain and river water forcing on the Bay of Bengal. *Journal of Geophysical Research* 121:2,425–2,446, http://dx.doi.org/10.1002/2015JC011325.

Benshila, R., F. Durand, S. Masson, R. Bourdallé-Badie, C. de Boyer Montégut, F. Papa, and G. Madec. 2014. The upper Bay of Bengal salinity structure in a high resolution model. *Ocean Modelling* 74:36–52, http://dx.doi.org/10.1016/j.ocemod.2013.12.001.

Brown, J.N., A. Sen Gupta, J.R. Brown, L.C. Muir, J.S. Risbey, P. Whetton, X. Zhang, B. Ganachaud, B. Murphy, and S.E. Wijffels. 2013. Implications of CMIP3 model biases and uncertainties for climate projections in the western tropical Pacific. *Climate Change* 119:147–161, http://dx.doi.org/10.1007/s10584-012-0603-5.

Chowdary, J.S., A. Parekh, S. Ojha, and C. Gnanaseelan, and R. Kakatkar. 2016a. Impact of upper ocean processes and air-sea fluxes on seasonal SST biases over the tropical Indian Ocean in the NCEP Climate Forecasting System. *International Journal of Climatology* 36:188–207, http://dx.doi.org/10.1002/joc.4336.

Chowdary, J.S., A. Parekh, G. Srinivas, C. Gnanaseelan, T.S. Fousiya, R. Khandekar, and M.K. Roxy. 2016b. Processes associated with the tropical Indian Ocean subsurface temperature bias in a coupled mode. *Journal of Physical Oceanography,* http://dx.doi.org/10.1175/JPO-D-15-0245.1.

Dai, A., and K.E. Trenberth. 2002. Estimates of freshwater discharge from continents: Latitudinal and seasonal variations. *Journal of Hydrometeorology* 3:660–687, http://dx.doi.org/10.1175/1525-7541(2002)003<0660:EOFDFC>2.0.CO;2.

Dai, A., T. Qian, K.E. Trenberth, and J.D. Milliman. 2009. Changes in continental freshwater discharge from 1948 to 2004. *Journal of Climate* 22:2,773–2,791, http://dx.doi.org/10.1175/2008JCLI2592.1.

de Boyer Montégut, C., G. Madec, A.S. Fischer, A. Lazar, and D. Iudicone. 2004. Mixed layer depth over the global ocean: An examination of profile data and a profile-based climatology. *Journal of Geophysical Research* 109, C12003, http://dx.doi.org/10.1029/2004JC002378.

Derber, J., and A. Rosati. 1989. A global oceanic data assimilation system. *Journal of Physical Oceanography* 19:1,333–1,347, http://dx.doi.org/10.1175/1520-0485(1989)019<1333:AGODAS>2.0.CO;2.

Durand, F., F. Papa, A. Rahman, and S.K. Bala. 2011. Impact of Ganga-Brahmaputra interannual discharge variations on Bay of Bengal salinity and temperature during 1992–1999 period. *Journal of Earth System Science* 120:859–872, http://dx.doi.org/10.1007/s12040-011-0118-x.

Durand, F., D. Shankar, F. Birol, and S.S.C. Shenoi. 2009. Spatiotemporal structure of the East India Coastal Current from satellite altimetry. *Journal of Geophysical Research* 114, C02013, http://dx.doi.org/10.1029/2008JC004807.

Fousiya, T.S., A. Parekh, and C. Gnanaseelan. 2015. Interannual variability of upper ocean stratification in Bay of Bengal: Observational and modeling aspects. *Theoretical and Applied Climatology* 1–17, http://dx.doi.org/10.1007/s00704-015-1574-z.

Fox-Kemper, B., G. Danabasoglu, R. Ferrari, S.M. Griffies, R.W. Hallberg, M.M. Holland, M.E. Maltrud, S. Peacock, and B.L. Samuels. 2011. Parameterization of mixed layer eddies: Part III. Implementation and impact in global ocean climate simulations. *Ocean Modelling* 39:61–78, http://dx.doi.org/10.1016/j.ocemod.2010.09.002.

Fox-Kemper, B., G. Danabasoglu, R. Ferrari, and R.W. Hallberg. 2008a. Parameterizing submesoscale physics in global climate models. *CLIVAR Exchanges* 13:3–5.

Fox-Kemper, B., R. Ferrari, and R.W. Hallberg. 2008b. Parameterization of mixed layer eddies: Part I. Theory and diagnosis. *Journal of Physical Oceanography* 38(6):1,145–1,165, http://dx.doi.org/10.1175/2007JPO3792.1.

Gadgil, S., P.V. Joseph, and N.V. Joshi. 1984. Ocean atmosphere coupling over monsoon regions. *Nature* 312:141–143, http://dx.doi.org/10.1038/312141a0.

Gill, A.E. 1982. *Atmosphere-Ocean Dynamics*. Academic Press, San Diego, 662 pp.

Graham, N.E., and T.P. Barnett. 1987. Sea surface temperature, surface wind divergence, and convection over tropical oceans. *Science* 238:657–659, http://dx.doi.org/10.1126/science.238.4827.657.

Griffies, S.M. 2012. *Elements of the Modular Ocean Model (MOM): 2012 Release*. GFDL Ocean Group Technical Report No. 7, Princeton, NJ, 631 pp.

Griffies, S.M., M.J. Harrison, R.C. Pacanowski, and A. Rosati. 2004. *A Technical Guide to MOM4*. GFDL Ocean Group Technical Report No. 5. Princeton, NJ, NOAA/Geophysical Fluid Dynamics Laboratory, 342 pp.

Howden, D.S., and R. Murtugudde. 2001. Effects of river inputs into the Bay of Bengal. *Journal of Geophysical Research* 106(C9):19,825–19,844, http://dx.doi.org/10.1029/2000JC000656.

Jinadasa, S.U.P., I. Lozovatsky, J. Planella-Morató, J.D. Nash, J.A. MacKinnon, A.J. Lucas, H.W. Wijesekera, and H.J.S. Fernando. 2016. Ocean turbulence and mixing around Sri Lanka and in adjacent waters of the northern Bay of Bengal. *Oceanography* 29(2):170–179, http://dx.doi.org/10.5670/oceanog.2016.49.

Jochum, M., G. Briegleb, G. Danabasoglu, W.G. Large, N.J. Norton, S.R. Jayne, M.H. Alford, and F.O. Bran. 2013. The impact of oceanic near-inertial waves on climate. *Journal of Climate* 26:2,833–2,844, http://dx.doi.org/10.1175/JCLI-D-12-00181.1.

Johnston, T.M.S., D. Chaudhuri, M. Mathur, D.L. Rudnick, D. Sengupta, H.L. Simmons, A. Tandon, and R. Venkatesan. 2016. Decay mechanisms of near-inertial mixed layer oscillations in the Bay of Bengal. *Oceanography* 29(2):180–191, http://dx.doi.org/10.5670/oceanog.2016.50.

Kanamitsu, M.W., J.W. Ebisuzaki, S.K. Yang, J.J. Hnilo, M. Fiorino, and G.L. Potter. 2002. NCEP-DEO AMIP-II reanalysis (R-2). *Bulletin of American Meteorological Society* 83:1,631–1,643, http://dx.doi.org/10.1175/BAMS-83-11-1631.

Kara, A.B., P.A. Rochford, and H.E. Hurlburt. 2003. Mixed layer depth variability over the global ocean. *Journal of Geophysical Research* 108(C3), 3079, http://dx.doi.org/10.1029/2000JC000736.

Large, W.G., J.C. McWilliams, and S.C. Doney. 1994. Oceanic vertical mixing: A review and a model with a nonlocal boundary layer parameterization. *Reviews of Geophysics* 32:363–403, http://dx.doi.org/10.1029/94RG01872.

Large, W., and S. Yeager. 2004. *Diurnal to Decadal Global Forcing for Ocean and Sea-Ice Models: The Data Sets and Flux Climatologies*. NCAR Technical Note: NCAR/TN-460+STR. CGD Division of the National Center for Atmospheric Research, 112 pp.

Locarnini, R.A., A.V. Mishonov, J.I. Antonov, T.P. Boyer, H.E. Garcia, O.K. Baranova, M.M. Zweng, C.R. Paver, J.R. Reagan, D.R. Johnson, and others. 2013. *World Ocean Atlas 2013, Volume 1: Temperature*. S. Levitus, ed., A. Mishonov, technical ed., NOAA Atlas NESDIS 73, 40 pp.

Lucas, A.J., J.D. Nash, R. Pinkel, J.A. MacKinnon, A. Tandon, A. Mahadevan, M.M. Omand, M. Freilich, D. Sengupta, M. Ravichandran, and A. Le Boyer. 2016. Adrift upon a salinity-stratified sea: A view of upper-ocean processes in the Bay of Bengal during the southwest monsoon. *Oceanography* 29(2):134–145, http://dx.doi.org/10.5670/oceanog.2016.46.

MacKinnon, J.A., L. St. Laurent, and A. Naveira Garabato. 2013. Diapycnal mixing processes in the ocean interior. Pp. 159–184 in *Ocean Circulation and Climate: A 21st Century Perspective*. G. Siedler, S. Griffies, J. Gould, and J. Church, eds, Academic Press.

Mahadevan, A., G. Spiro Jaeger, M. Freilich, M. Omand, E.L. Shroyer, and D. Sengupta. 2016. Freshwater in the Bay of Bengal: Its fate and role in air-sea heat exchange. *Oceanography* 29(2):72–81, http://dx.doi.org/10.5670/oceanog.2016.40.

Marshall, J., A. Adcroft, C. Hill, L. Perelman, and C. Heisey. 1997. A finite-volume, incompressible Navier-Stokes model for studies of the ocean on parallel computers. *Journal of Geophysical Research* 102(C3):5,753–5,766.

McPhaden, M.J. 1993. TOGA-TAO and the 1991–93 El Niño-Southern Oscillation event. *Oceanography* 6(2):36–44, http://dx.doi.org/10.5670/oceanog.1993.12.

McPhaden, M.J., G. Meyers, K. Ando, Y. Masumoto, V.S.N. Murty, M. Ravichandran, F. Syamsudin, J. Vialard, L. Yu, and W. Yu. 2009. RAMA: The Research Moored Array for African-Asian-Australian Monsoon Analysis and Prediction. *Bulletin of American Meteorological Society* 90:459–480, http://dx.doi.org/10.1175/2008BAMS2608.1.

Narvekar, J., and S. Prasanna Kumar. 2006. Seasonal variability of the mixed layer in the central Bay of Bengal and associated changes in nutrients and chlorophyll. *Deep Sea Research Part I* 53:820–835, http://dx.doi.org/10.1016/j.dsr.2006.01.012.

Menemenlis, D., J.M. Campin, P. Heimbach, C. Hill, T. Lee, A. Nguyen, M. Schodlock, and H. Zhang. 2008. ECCO2: High resolution global ocean and sea ice data synthesis. *Mercator Ocean Quarterly Newsletter* #31:13–21, http://ecco2.org/manuscripts/reports/ECCO2_Mercator.pdf.

Packnowski, R.C., and S.G.H. Philander. 1981. Parameterization of vertical mixing in numerical models of the tropical ocean. *Journal of Physical Oceanography* 11:1,442–1,451, http://dx.doi.org/10.1175/1520-0485(1981)011<1443:POVMIN>2.0.CO;2.

Pan, H.L., and W.S. Wu. 1995. *Implementing a Mass Flux Convective Parameterization Package for the NMC Medium-Range Forecast Model*. NOAA National Meteorological Center Office Note 409, 40 pp.

Papa, F., C. Prigent, F. Aires, C. Jimenez, W.B. Rossow, and E. Matthews. 2010. Interannual variability of surface water extent at global scale. *Journal of Geophysical Research* 115, D12111, http://dx.doi.org/10.1029/2009JD012674.

Parekh, A., J.S. Chowdary, O. Sayantani, T. Fousiya, and C. Gnanaseelan. 2016. Tropical Indian Ocean surface salinity bias in Climate Forecasting System coupled models and the role of upper ocean processes. *Climate Dynamics* 46:2,403–2,422, http://dx.doi.org/10.1007/s00382-015-2709-8.

Prasad, T.G. 1997. Annual and seasonal mean buoyancy fluxes for the tropical Indian Ocean. *Current Science* 73:667–674.

Praveen Kumar, B., J. Vialard, M. Lengaigne, V.S.N. Murty, and M.J. McPhaden. 2010. TropFlux: Air-sea fluxes for the global tropical oceans: Description and evaluation against observations. *Climate Dynamics* 38:1,521–1,543, http://dx.doi.org/10.1007/s00382-011-1115-0.

Rahaman, H., M. Ravichandran, D. Sengupta, M.J. Harrison, and S.M. Griffies. 2014. Development of a regional model for the North Indian Ocean. *Ocean Modelling* 75:1–19, http://dx.doi.org/10.1016/j.ocemod.2013.12.005.

Rao, R.R., and R. Sivakumar. 1999. On the possible mechanisms of the evolution of a mini-warm pool during the pre-summer monsoon season and the genesis of onset vortex in the southeastern Arabian Sea. *Quarterly Journal of Royal Meteorological Society* 125:787–809, http://dx.doi.org/10.1002/qj.49712555503.

Rao, R.R., and R. Sivakumar. 2003. Seasonal variability of sea surface salinity and salt budget of the mixed layer of the north Indian Ocean. *Journal of Geophysical Research* 108(C1), 3009, http://dx.doi.org/10.1029/2001JC000907.

Ravichandran, M., D. Behringer, S. Sivareddy, M.S. Girishkumar, N. Chacko, and R. Harikumar. 2013. Evaluation of the Global Ocean Data Assimilation System at INCOIS: The Tropical Indian Ocean. *Ocean Modelling* 69:123–135, http://dx.doi.org/10.1016/j.ocemod.2013.05.003.

Roxy, M. 2014. Sensitivity of precipitation to sea surface temperature over the tropical summer monsoon region and its quantification. *Climate Dynamics* 43:1,159–1,169, http://dx.doi.org/10.1007/s00382-013-1881-y.

Saha, S., S. Moorthi, X. Wu, J. Wang, S. Nadiga, P. Tripp, D. Behringer, Y.-T. Hou, H-y. Chuang, M. Iredell, and others. 2014. The NCEP Climate Forecast System Version 2. *Journal of Climate* 27:2,185–2,208, http://dx.doi.org/10.1175/JCLI-D-12-00823.1.

Saha, S., S. Nadiga, C. Thiaw, J. Wang, W. Wang, Q. Zhang, H.M. Van den Dool, H.-L. Pan, S. Moorthi, D. Behringer, and others. 2006. The NCEP Climate Forecast System. *Journal of Climate* 19:3,483–3,517, http://dx.doi.org/10.1175/JCLI3812.1.

Sahai, A.K., S. Sharmila, S. Abhilash, R. Chattopadhyay, N. Borah, R.P.M. Krishna, J. Susmitha, M. Roxy, S. De, and S. Pattnaik. 2013. Simulation and extended range prediction of monsoon intraseasonal oscillations in NCEP CFS/GFS version 2 framework. *Current Science* 104:1,394–1,408.

Sanilkumar, K., N. Mohankumar, M. Joseph, and R. Rao. 1994. Genesis of meteorological disturbances and thermohaline variability of the upper layers in the head of the Bay of Bengal during Monsoon Trough Boundary Layer Experiment (MONTBLEX-90). *Deep Sea Research Part I* 41:1,569–1,581, http://dx.doi.org/10.1016/0967-0637(94)90061-2.

Sarkar, S., H.T. Pham, S. Ramachandran, J.D. Nash, A. Tandon, J. Buckley, A.A. Lotliker, and M.M. Omand. 2016. The interplay between submesoscale instabilities and turbulence in the surface layer of the Bay of Bengal. *Oceanography* 29(2):146–157, http://dx.doi.org/10.5670/oceanog.2016.47.

Schott, F., and J.P. McCreary. 2001. The monsoon circulation of the Indian Ocean. *Progress in Oceanography* 51:1–123, http://dx.doi.org/10.1016/S0079-6611(01)00083-0.

Sengupta, D., G.N. Bharath Raj, M. Ravichandran, J. Sree Lekha, and F. Papa. 2016. Near-surface salinity and stratification in the north Bay of Bengal from moored observations. *Geophysical Research Letters* 43:4,448–4,456, http://dx.doi.org/10.1002/2016GL068339.

Sengupta, D., G.N. Bharath Raj, and S.S.C. Shenoi. 2006. Surface freshwater from Bay of Bengal runoff and Indonesian throughflow in the tropical Indian Ocean. *Geophysical Research Letters* 33, L22609, http://dx.doi.org/10.1029/2006GL027573.

Servain, J., A. Busalacchi, M.J. McPhaden, A.D. Moura, G. Reverdin, M. Vianna, and S. Zebiak. 1998. A Pilot Research Moored Array in the Tropical Atlantic (PIRATA). *Bulletin of the American Meteorology Society* 79:2,019–2,031, http://dx.doi.org/10.1175/1520-0477(1998)079<2019:APRMAI>2.0.CO;2.

Seo, H., S.P. Xie, R. Murtugudde, M. Jochum, and A.J. Miller. 2009. Seasonal effects of Indian Ocean freshwater forcing in a regional coupled model. *Journal of Climate* 22:6,577–6,596, http://dx.doi.org/10.1175/2009JCLI2990.1.

Shankar, D., P.N. Vinayachandran, and A.S. Unnikrishnan. 2002. The monsoon currents in the north Indian Ocean. *Progress in Oceanography* 52:63–120, http://dx.doi.org/10.1016/S0079-6611(02)00024-1.

Shenoi, S.S.C., D. Shankar, and S.R. Shetye. 2002. Differences in heat budgets of the near surface Arabian Sea and Bay of Bengal: Implications for the summer monsoon. *Journal of Geophysical Research* 107, 3052, http://dx.doi.org/10.1029/2000JC000679.

Subramanian, V. 1993. Sediment load of Indian rivers. *Current Science* 64:928–930.

Thompson, B., C. Gnanaseelan, and P.S. Salvekar. 2006. Variability in the Indian Ocean circulation and salinity and its impact on SST anomalies during dipole events. *Journal of Marine Research* 64:853–880, http://dx.doi.org/10.1357/002224006779698350.

Venkatesan, R., V.R. Shamji, G. Latha, S. Mathew, R.R. Rao, A. Muthiah, and M.A. Atmanand. 2013. In situ ocean subsurface time-series measurements from OMNI buoy network in the Bay of Bengal. *Current Science* 104(9):1,166–1,177.

Vinayachandran, P.N., J.P. McCreary, R.R. Hood, and K.E. Kohler. 2005. A numerical investigation of the phytoplankton bloom in the Bay of Bengal during northeast monsoon. *Journal of Geophysical Research* 110, C12001, http://dx.doi.org/10.1029/2005JC002966.

Vinayachandran, P.N., and R.S. Nanjundiah. 2009. Indian Ocean sea surface salinity variations in a coupled model. *Climate Dynamics* 33:245–263, http://dx.doi.org/10.1007/s00382-008-0511-6.

Vinayachandran, P.N., D. Shankar, S. Vernekar, K.K. Sandeep, P. Amol, C.P. Neema, and A. Chatterjee. 2013. A summer monsoon pump to keep the Bay of Bengal salty. *Geophysical Research Letters* 40:1,777–1,782, http://dx.doi.org/10.1002/grl.50274.

Wijesekera, H.W., E. Shroyer, A. Tandon, M. Ravichandran, D. Sengupta, S.U.P. Jinadasa, H.J.S. Fernando, N. Agrawal, K. Arulanathan, G.S. Bhat, and others. In press. ASIRI: An Ocean-Atmosphere Initiative for Bay of Bengal. *Bulletin of the American Meteorological Society*, http://dx.doi.org/10.1175/BAMS-D-14-00197.1.

Wilson, E.A., and S.C. Riser. 2016. An assessment of the seasonal salinity budget for the upper Bay of Bengal. *Journal of Physical Oceanography* 46(5):1,361–1,376, http://dx.doi.org/10.1175/JPO-D-15-0147.1.

Zweng, M.M., J.R. Reagan, J.I. Antonov, R.A. Locarnini, A.V. Mishonov, T.P. Boyer, H.E. Garcia, O.K. Baranova, D.R. Johnson, D. Seidov, and M.M. Biddle. 2013. *World Ocean Atlas 2013, Volume 2: Salinity*. S. Levitus, ed., A. Mishonov, technical ed., NOAA Atlas NESDIS 74, 39 pp.

AUTHORS

Jasti S. Chowdary is Scientist, Indian Institute of Tropical Meteorology, Pune, India. **G. Srinivas** is Scientist, Indian Institute of Tropical Meteorology, Pune, India. **T.S. Fousiya** is a graduate student at the Indian Institute of Tropical Meteorology, Pune, India. **Anant Parekh** is Scientist, Indian Institute of Tropical Meteorology, Pune, India. **C. Gnanaseelan** (seelan@tropmet.res.in) is Scientist, Indian Institute of Tropical Meteorology, Pune, India. **Hyodae Seo** is Associate Scientist, Woods Hole Oceanographic Institution, Woods Hole, MA, USA. **Jennifer A. MacKinnon** is Professor, Scripps Institution of Oceanography, University of California, San Diego, La Jolla, CA, USA.